J|A|C|S
ARTICLES
Published on Web 09/27/2005

# Heme Carbonyls: Environmental Effects on $\nu_{C-O}$ and Fe−C/C−O Bond Length Correlations

Nathan J. Silvernail,[†] Arne Roth,[†] Charles E. Schulz,*[,‡] Bruce C. Noll,[†] and W. Robert Scheidt*[,†]

*Contribution from the Department of Chemistry and Biochemistry, University of Notre Dame, Notre Dame, Indiana 46556, and Department of Physics, Knox College, Galesburg, Illinois, 61401*

Received May 13, 2005; E-mail: scheidt.1@nd.edu

***Abstract:*** The synthesis and characterization of four low-spin (carbonyl)iron(II) tetraphenylporphyrinates, [Fe(TPP)(CO)(L)], where L = 1-methylimidazole, 2-methylimidazole, 1,2-dimethylimidazole (unsolvated), and 1,2-dimethylimidazole (toluene solvate) are reported. The complexes show nearly the same value of $\nu_{C-O}$ in toluene solution (1969−72 $cm^{-1}$) but a large range of CO stretching frequencies in the solid-state (1926−1968 $cm^{-1}$). The large solid-state variation results from CO interactions in the solid state, as shown by an examination of the crystal structures of the four complexes. The high precision of the four structures obtained allows us to make a number of structural and spectroscopic correlations that describe the Fe−C−O and $N_{Im}$-Fe−CO units. The values of $\nu_{C-O}$ and the Fe−C and C−O bond distances are strongly correlated and provide a structural, as well as a spectroscopic, correlation of the $\pi$ back-bonding model. The interactions of CO described are closely related to the large range of CO stretching frequencies observed in heme proteins and specific interactions observed in carbonylmyoglobin (MbCO).

## Introduction

Studies involving the carbonyl (CO)[1] ligand have had a profound influence in both classical inorganic and organometallic chemistry, as well as bioinorganic chemistry systems, such as the iron porphyrinate (heme) carbonyls. The carbonyl ligand has been used to probe the nature of metal−ligand bonding and to provide information on the nature of the environment of prosthetic groups in proteins. For inorganic carbonyl derivatives, it has long been noted that there is a relationship between the strength of the metal−carbon bond and that of the carbon−oxygen bond.[2] The overall bonding interaction is that any feature that leads to strengthening the C−O bond concomitantly leads to a weakening of the metal−carbon bond. This is the basis of the so-called $\pi$-back-bonding model that is widely applied as a general model for bonding in complexes with $\pi$-acceptor ($\pi$-acid) ligands. This correlation has been extensively studied by vibrational spectroscopy; the trends observed in isoelectronic series of carbonyl species are a well-known phenomenon.[3] In heme carbonyl derivatives, trends in the Fe−C−O unit vibrations have long been established and are known as the "inverse correlation" of the iron−carbon stretching frequency ($\nu_{Fe-CO}$) and the carbon−oxygen stretching frequency ($\nu_{C-O}$).[4,5] An increase in the Fe−C bond order is seen to lead to a decrease in the C−O bond order.

Vibrational spectroscopy has been used since the inception of bioinorganic chemistry to study protein active sites. Vibrational spectroscopic techniques such as infrared (IR),[6] resonance Raman (rR),[7] and nuclear resonance vibrational spectroscopy (NRVS),[8] allow the use of diatomic probe ligands to study bonding and the environment near the binding site in metal-containing proteins.

The diatomic ligands CO, $CN^-$, NO, and $O_2$ all display ligand stretches that can be observed with vibrational techniques and have been extensively employed in the study of hemes and heme proteins.[7−13] The CO ligand has a high affinity for iron(II)

* To whom correspondence should be addressed: E-mail Scheidt.1@nd.edu (W.R.S.); Fax (574) 631−4044 (W.R.S.).
[†] University of Notre Dame.
[‡] Knox College.

(1) The following abbreviations are used in this paper. Proteins: Mb, myoglobin; MbCO, myoglobin with coordinated CO; Hb, hemoglobin; HbCO, hemoglobin with coordinated CO. Porphyrins: Por, generalized porphyrin dianion; OEP, dianion of octaethylporphyrin; Deut, dianion of deuteroporphyrin; TpivPP, dianion of *meso*-α,α,α,α-tetrakis(*o*-pivalamidophenyl)porphyrin; TPP, dianion of *meso*-tetraphenylporphyrin. Ligands: Im, generalized imidazole; 1-MeIm, 1-methylimidazole; 2-MeHIm, 2-methylimidazole; 1,2-$Me_2$Im, 1,2-dimethylimidazole; $SEt^-$, anion of ethanethiol; THF, tetrahydrofuran; THT, tetrahydrothiophene; Py, pyridine. Spectroscopic techniques: IR, infrared absorption spectroscopy; rR, resonance Raman spectroscopy; NRVS, nuclear resonance vibrational spectroscopy.

(2) Cotton, F. A.; Wilkinson, G.; Murillo, C. A.; Bochmann, M. *Advanced Inorganic Chemistry*, 6th ed.; Wiley and Sons: New York, 1999; pp 636−639.
(3) Nakamoto, K. *Infrared and Raman Spectra of Inorganic and Coordination Compounds*, 3rd ed.; Wiley and Sons: New York, 1978; pp 279−281.
(4) Tsubaki, M.; Ichikawa, Y. *Biochim. Biophys. Acta* **1985**, *827*, 268.
(5) Uno, T.; Nishimura, Y.; Masamichi, T.; Makino, R.; Iizuka, T.; Ishimura, Y. *J. Biol. Chem.* **1987**, *262*, 4549.
(6) Alben, J. O.; Fiamingo, F. G. In *Optical Techniques in Biological Research*; Rousseau, D. L., Ed.; Academic Press: Orlando, 1984; pp 133−179.
(7) (a) Rousseau, D. L.; Ondrias, M. R. In *Optical Techniques in Biological Research*; Rousseau, D. L., Ed.; Academic Press: Orlando, 1984; pp 65−132. (b) Kerr, E. A.; Yu, N. T. *Biological Applications of Raman Spectroscopy*; Spiro, T. G., Ed.; Wiley and Sons: New York, 1988; Vol. 3, pp 39−95.
(8) Scheidt, W. R.; Durbin, S. M.; Sage, J. T. *J. Inorg. Biochem.* **2005**, *99*, 60.
(9) Wang, J. H.; Nakahara, A.; Fleischer, E. B. *J. Am. Chem. Soc.* **1958**, *80*, 1109.


10.1021/ja053148x CCC: $30.25 

hemes,[9,14−17] and $\nu_{C-O}$ is conveniently observed.[13] Consequently, CO has been widely used as a probe ligand to detect vacant coordination sites in reduced heme proteins. Carbon monoxide is also an interesting biomolecule that is a product of heme catabolism. Accordingly, the background body burden of CO is relatively high.[18] Since CO has a higher binding constant than that of dioxygen, this natural CO level is potentially toxic. Nature has solved the toxicity problem by designing factors into the heme proteins hemoglobin (Hb) and myoglobin (Mb) so that their CO affinity is reduced by approximately 2 orders of magnitude compared to that of analogous iron(II) porphyrinates.[19,20]

The origin of the molecular basis of the differences (selectivity) in the $O_2$ and CO affinities between the heme proteins and low-molecular-weight hemes has been an intensively studied problem in bioinorganic chemistry. An early prominent idea was that the environment of the protein ligand binding pocket somehow imposes constraints on the Fe−C−O unit but not on the Fe−O−O unit. There has been much discussion about possible geometric constraints of the Fe−C−O unit in MbCO.[10,21−25] Although a number of protein crystal structures have supported a rather bent Fe−C−O unit,[26−29] more recent results do not.[30,31] Additionally, polarized IR photoselection measurements on Mb single crystals and in solution support an only slightly bent Fe−C−O unit.[24,25] The original idea of geometric constraints imposed by the protein has largely shifted to investigations of the global (electrostatic) environment near the CO binding site.[23] CO has been widely used to investigate the specific and global (electrostatic) environment.

The heme proteins myoglobin and hemoglobin have been among the most studied CO-ligated proteins. In the CO derivatives of native Mb and Hb, up to four distinct CO stretching frequencies can be observed.[32,33] These bands have been designated $A_0$, $A_1$, $A_2$, and $A_3$ in Mb. This range of frequencies has been attributed to varying conformational, and subsequently, electrostatic environments in the heme pocket.[34−36] A complete understanding of these bands is of interest since they provide information about the relationship of conformational substates with functional states of the protein.[23−29,69] A large number of mutation studies have been dedicated to understanding the multiple-peak phenomenon, differing environ-


(10) Spiro, T. G.; Zgierski, M. Z.; Kozlowski, P. W. *Coord. Chem. Rev.* **2001**, *219−221*, 923.
(11) Kitagawa, T.; Ozaki, Y. *Struct. Bonding (Berlin)* **1987**, *64*, 71.
(12) Alben, J. O. In *The Porphyrins*; Dolphin, D., Ed.; Academic Press: New York, 1978; Vol. 3, pp 323−345.
(13) Caughey, W. S.; Alben, J. O. *Biochemistry* **1968**, *7*, 175.
(14) Li, T.; Quillin, M. L.; Phillips, G. N., Jr.; Olsen, J. S. *Biochemistry* **1994**, *33*, 1433.
(15) Rougee, M.; Brault, D. *Biochemistry* **1975**, *14*, 4100.
(16) Rougee, M.; Brault, D. *Biochem. Biophys. Res. Commun.* **1974**, *57*, 654.
(17) Gibson, Q. H.; Roughton, F. J. *Proc. R. Soc., Ser. B, Biol. Sci.* **1957**, *146*, 206.
(18) Landaw, S. A.; Callahan, E. W., Jr.; Schmid, R. *J. Clin. Invest.* **1970**, *49*, 914.
(19) Collman, J. P.; Brauman, J. I.; Halbert, T. R.; Suslick, K. S. *Proc. Natl. Acad. Sci. U.S.A.* **1976**, *73*, 3333.
(20) Antonini, E.; Brunori, M. *Hemoglobin and Myoglobin in Their Reactions With Ligands*; North-Holland: London, 1971.
(21) Spiro, T. G.; Smulevich, G.; Su, C. *Biochemistry* **1990**, *29*, 4497.
(22) (a) Jewsbury, P.; Yamamoto, S.; Minato, T.; Saito, Minoru, S.; Kitagawa, T. *J. Am. Chem. Soc.* **1994**, *116*, 11586. (b) Jewsbury, P.; Yamamoto, S.; Minato, T.; Saito, Minoru, S.; Kitagawa, T. *J. Phys. Chem.* **1995**, *99*, 12677.
(23) Springer, B. A.; Sligar, S. G.; Olsen, J. S.; Phillips, G. N., Jr. *Chem. Rev.* **1994**, *94*, 699.
(24) Ivanov, D.; Sage, J. T.; Keim, M.; Powell, J. R.; Asher, S. A.; Champion, P. M. *J. Am. Chem. Soc.* **1994**, *116*, 4139.
(25) Lim, M.; Jackson, T. A.; Anfinrud, P. A. *Science.* **1995**, *269*, 962.
(26) Kuriyan, J.; Wilz, S.; Karplus, M.; Petsko, G. A. *J. Mol. Biol.* **1986**, *192*, 133.
(27) Teng, T.-Y.; Šrajer, V.; Moffat, K. *Nat. Struct. Biol.* **1994**, *1*, 701.
(28) Schlichting, I.; Berendzen, J.; Phillips, G. N., Jr.; Sweet, R. M. *Nature* **1994**, *371*, 808.
(29) Cheng, X.; Schoenborn, B. P. *J. Mol. Biol.* **1991**, *220*, 381.
(30) Vojtechovský, J.; Chu, K.; Berendzen, J.; Sweet, R. M.; Schlichting, I. *Biophys. J.* **1999**, *77*, 2153.
(31) Kachalova, G. S.; Popov, A. N.; Bartunik, H. D. *Science* **1999**, *284*, 473.
(32) Shimada, H.; Caughey, W. S. *J. Biol. Chem.* **1982**, *257*, 11893.
(33) Potter, W. T.; Hazzard, J. H.; Choc, M. G.; Tucker, M. P.; Caughey, W. S. *Biochemistry* **1990**, *29*, 6283.
(34) Frauenfelder, H.; Sligar, S. G.; Wolynes, P. G. *Science* **1991**, *254*, 1598. Young, R. D.; Frauenfelder, H.; Johnson, J. B.; Lamb, D. C.; Nienhaus, G. U.; Phillip, R.; Scholl, R. *Chem. Phys.* **1991**, *158*, 315.
(35) Alben, J. O.; Beece, D.; Bowne, S. F.; Doster, W.; Eisenstein, L.; Frauenfelder, H.; Good, D.; McDonald, M. C.; Marden, M. C.; Moh, P. P.; Reinisch, L.; Reynolds, A. H.; Shyamsunder, E.; Yue, K. T. *Proc. Natl. Acad. Sci. U.S.A.* **1982**, *79*, 3744.
(36) Makinen, M. W.; Houtchens, R. A.; Caughey, W. S. *Proc. Natl. Acad. Sci. U.S.A.* **1979**, *76*, 6042.
(37) Phillips, G. N., Jr.; Teodoro, M. L.; Li, T.; Smith, B.; Olsen, J. S. *J. Phys. Chem. B* **1999**, *103*, 8817.
(38) Adler, A. D.; Longo, F. R.; Finarelli, J. D.; Goldmacher, J.; Assour, J.; Korsakoff, L. *J. Org. Chem.* **1967**, *32*, 476.
(39) Adler, A. D.; Longo, F. R.; Kampus, F.; Kim, J. *J. Inorg. Nucl. Chem.* **1970**, *32*, 2443.
(40) (a) Fleischer, E. B.; Srivastava, T. S. *J. Am. Chem. Soc.* **1969**, *91*, 2403. (b) Hoffman, A. B.; Collins, D. M.; Day, V. W.; Fleischer, E. B.; Srivastava, T. S.; Hoard, J. L. *J. Am. Chem. Soc.* **1972**, *94*, 3620.
(41) Stolzenberg, A. M.; Strauss, S. H.; Holm, R. H. *J. Am. Chem. Soc.* **1981**, *103*, 4763.
(42) Sheldrick, G. M. *Program for empirical absorption correction of area detector data*; Universität Göttingen: Göttingen, Germany, 1996.
(43) Sheldrick, G. M. *Acta Crystallogr.* **1990**, *A46*, 467.
(44) Patterson, A. L. *Phys. Rev.* **1934**, *46*, 372.
(45) Sheldrick, G. M. *SHELXL-97: FORTRAN program for crystal structure refinement*; Universität Göttingen: Göttingen, Germany, 1997.
(46) A reviewer has raised the question of possible problems with correlation of the parameters in the disordered system. We have carried out three types of refinement of the disordered imidazole. The first was the "traditional" refinement with constrained imidazole ring and equivalent Fe−N bond distances. We also carried out two refinements with unconstrained axial Fe−N bonds, one with constrained imidazole ring parameters and the second with free imidazole ring parameters. These two refinements gave essentially the same Fe−N distances and occupancies of the two rings. We concluded that there was a real chance that the two ring orientations and differing Fe−N distances was the correct choice to be made for this particular problem, which is clearly a difficult one.
(47) Salzmann, R.; Ziegler, C. J.; Godbout, N.; McMahon, M. T.; Suslick, K. S.; Oldfield, E. *J. Am. Chem. Soc.* **1998**, *120*, 11323.
(48) Silvernail, N. J.; Noll, B. C.; Scheidt, W. R. unpublished results.
(49) White, D. K.; Cannon, J. B.; Traylor, T. G. *J. Am. Chem. Soc.* **1979**, *101*, 2443.
(50) Collman, J. P.; Brauman, J. I.; Doxsee, K. M.; Halbert T. R.; Suslick, K. S. *Proc. Natl. Acad. Sci. U.S.A.* **1978**, *75*, 564.
(51) Little. R. G.; Ibers, J. A. *J. Am. Chem. Soc.* **1974**, *96*, 4452.
(52) Kim, K.; Ibers, J. A. *J. Am. Chem. Soc.* **1991**, *113*, 6077.
(53) Slebodnick, C.; Duval, M. L.; Ibers, J. A. *Inorg. Chem.* **1996**, *35*, 3607.
(54) Hashimoto, T.; Dyer, R. L.; Crossley, M. J.; Baldwin, J. E.; Basolo, F. *J. Am. Chem. Soc.* **1982**, *104*, 2101.
(55) Ricard, L.; Weiss, R.; Momenteau, M. *J. Chem. Soc., Chem. Commun.* **1986**, 818.
(56) Collman, J. P.; Sorrell, T. N. *J. Am. Chem. Soc.* **1975**, *97*, 4133.
(57) Salzmann, R.; McMahon, M. T.; Godbout, N.; Sanders, L. K.; Wojdelski, M.; Oldfield, E. *J. Am. Chem. Soc.* **1999**, *121*, 3818.
(58) Slebodnick, C.; Fettinger, J. C.; Peterson, H. B.; Ibers, J. A. *J. Am. Chem. Soc.* **1996**, *118*, 3216.
(59) Kim, K.; Fettinger, J. C.; Sessler, J. L.; Cyr, M.; Hugdahl, J.; Collman, J. P.; Ibers, J. A. *J. Am. Chem. Soc.* **1989**, *111*, 403.
(60) Peng, S. M.; Ibers, J. A. *J. Am. Chem. Soc.* **1976**, *98*, 8032.
(61) Buchler, J. W.; Kokisch, W.; Smith, P. D. *Struct. Bonding (Berlin)* **1978**, *34*, 79.
(62) Scheidt, W. R.; Haller, K. J.; Fons, M.; Mashiko, T.; Reed, C. A. *Biochemistry* **1981**, *20*, 3653.
(63) Collman, J. P.; Sorrel, T. N.; Dawson, J. H.; Trudell, J. R.; Bunnenberg, E.; Djerassi, C. *Proc. Natl. Acad. Sci. U.S.A.* **1976**, *73*, 6.
(64) Caron, C.; Mitschler, A.; Rivére, G.; Richard, L.; Schappacher, M.; Weiss, R. *J. Am. Chem. Soc.* **1979**, *101*, 7401.
(65) Momenteau, M.; Scheidt, W. R.; Eigenbrot, C. W.; Reed, C. A. *J. Am. Chem. Soc.* **1988**, *110*, 1207.
(66) Munro, O. Q.; Marques, H. M.; Debrunner, P. G.; Mohanrao, K.; Scheidt, W. R. *J. Am. Chem. Soc.* **1995**, *117*, 935.
(67) Several bis-ligated iron(II) complexes of general formula $[Fe(Por)(L)_2]$, where L is an imidazole derivative, have been structurally characterized. The values of Fe−N(L) are as follows (a) $[Fe(TPP)(1\text{-}MeIm)_2]$, 2.014(5) Å, Hoard, J. L. personal communication to W.R.S.; (b) $[Fe(TPP)(1\text{-}VinIm)_2]$, 2.004(2) Å; $[Fe(TPP)(1\text{-}BzIm)_2]$, 2.017(4), Safo, M. K.; Scheidt, W. R.; Gupta, G. P. *Inorg. Chem.* **1990**, *29*, 626.
(68) Cao, C.; Dahal, S.; Shang, M.; Beatty, A. M.; Hibbs, W.; Schulz, C. E.; Scheidt, W. R. *Inorg. Chem.***2003**, *42*, 5202.
(69) Scheidt, W. R.: Piciulo, P. L. *J. Am. Chem. Soc.* **1976**, *98*, 1913.

ments, and substrate selectivity (CO vs $O_2$) in myoglobin.[14,37] These investigations have demonstrated that CO frequency changes can be the result of very specific interactions with ligand pocket residues or the general electrostatic environment of the pocket or both.

In this paper, we present the synthesis, spectroscopic, and structural studies for four new carbonyl(iron(II)) tetraphenylporphyrinates, each with an imidazole as the sixth ligand. The complexes are of the form [Fe(TPP)(CO)(L)], where L is 2-methylimidazole, 1,2-dimethylimidazole (two crystalline forms), or 1-methylimidazole. The crystals of all four compounds are of extremely high quality and allowed the determination of the structural parameters at very high levels of accuracy. Although the species show nearly identical CO stretching frequencies in solution, the crystalline species show a wide range of $\nu_{C-O}$ values. The variation in the solid-state $\nu_{C-O}$ values have been examined in light of the differing crystalline environments. These provide information on the nature of some of the environmental effects that can lead to shifts in $\nu_{C-O}$. These compounds also provide additional, quantitative data on classical carbonyl−metal $\pi$-bonding. There are differences in both the Fe−C and C−O bond lengths in the four compounds. Although the differences are relatively small, the structure determinations show that there is a strong correlation between the two distances that follows the indirect correlation, i.e., an increase in the Fe−C distance leads to a decrease in the C−O distance. The observed structural correlation appears to be consistent with other carbonyl species whose structural data was determined with lower accuracy and precision.

## Experimental Section

**General Information.** All reactions were carried out under strictly anaerobic conditions using standard Schlenk techniques under an argon atmosphere. Ethanethiol and 1-methylimidazole were used as received (Acros). 2-Methylimidazole (Aldrich) was recrystallized from acetone prior to use. 1,2-Dimethylimidazole (Aldrich) was recrystallized from ethyl ether prior to use. Carbon monoxide gas was used as received (Mittler Specialty Gases). Benzene and toluene (Fisher) were purified by distillation in a nitrogen atmosphere over sodium/benzophenone ketyl. All solvents were freeze/pump/thaw degassed (thrice) prior to use. Free base [$H_2$TPP] was prepared according to Adler et al.[38] [Fe(TPP)(Cl)] was prepared according to the metalation procedure of Adler et al.[39] [Fe(TPP)]$_2$O was prepared by washing a solution of [Fe(TPP)Cl] in methylene chloride with 2 M aqueous sodium hydroxide solution (3×) and drying the collected organic layers over magnesium sulfate followed by recrystallization from methylene chloride/hexanes.[40] [Fe(TPP)] was prepared by stirring a solution of [Fe(TPP)]$_2$O and excess ethanethiol in benzene for 2 d.[41] After reduction, solvent and excess ethanethiol were removed under vacuum.

Infrared spectra were recorded on a Nicolet Nexus 870 FT-IR spectrometer. Solid-state infrared samples were prepared by gently mulling a suitable crystal between two NaCl plates with a small amount of Nujol to allow dispersion. Solution infrared samples were prepared by bubbling CO into a solution of 4 mM Fe(TPP) and 1−2 M imidazole in toluene. Samples were prepared for Mössbauer spectroscopy by weighing approximately 40 mg of selected crystals, grinding them in a small volume of Apiezon M grease to form a mull, and placing them into a Mössbauer cup. Measurements were performed on a constant-acceleration spectrometer from 15 to 300 K.

**Synthesis of [Fe(TPP)(CO)(1,2-Me$_2$Im)]·C$_7$H$_8$.** A solution of 29 mg (0.30 mmol) of 1,2-dimethylimidazole, in 6 mL of toluene, was introduced to dry [Fe(TPP)] (0.04 mmol) via cannula transfer and stirred for 1 h. The reaction solution was then purged with CO for 30 min and stirred overnight under a CO atmosphere. The solution was then cannula-transferred into 7 mm glass tubes, carefully layered with hexanes, and the tubes were flame sealed. X-ray quality crystals of [Fe(TPP)(CO)(1,2-Me$_2$Im)]·C$_7$H$_8$ were isolated after 48 h at 4°C. IR $\nu_{CO}$ in KBr: 1953 and 1948 cm$^{-1}$.

**Synthesis of [Fe(TPP)(CO)(2-MeHIm)]·C$_7$H$_8$.** A solution of 35 mg (0.40 mmol) of 2-methylimidazole, in 6 mL of toluene, was introduced to dry [Fe(TPP)] (0.05 mmol) via cannula transfer and stirred for 1 h. The reaction solution was then purged with CO for 30 min and stirred overnight under a CO atmosphere. The solution was then cannula-transferred into 7 mm glass tubes, carefully layered with hexanes, and the tubes were flame sealed. X-ray quality crystals of [Fe(TPP)(CO)(2-MeHIm)]·C$_7$H$_8$ were isolated after 48 h at 4°C. IR $\nu_{CO}$ in KBr: 1926 cm$^{-1}$.

**Synthesis of [Fe(TPP)(CO)(1,2-Me$_2$Im)].** A solution of 52 mg (0.53 mmol) of 1,2-dimethylimidazole in 5 mL of toluene, was introduced to dry [Fe(TPP)] (0.13 mmol) via cannula transfer and stirred for 1 h. The reaction solution was then purged with CO for 30 min and stirred overnight under a CO atmosphere. The solution was then cannula-transferred into 8 mm glass tubes, carefully layered with hexanes, and the tubes were flame sealed. X-ray quality crystals of [Fe(TPP)(CO)(1,2-Me$_2$Im)] were isolated after 25 days at 25 °C. IR $\nu_{CO}$ in KBr: 1963 cm$^{-1}$.

**Synthesis of [Fe(TPP)(CO)(1-MeIm)]·C$_6$H$_6$.** A solution of 0.08 mL (0.94 mmol) of 1-methylimidazole, in 15 mL of benzene, was introduced to dry [Fe(TPP)] (0.26 mmol) via cannula transfer and stirred for 1 h. The reaction solution was then purged with CO for 30 min and stirred overnight under a CO atmosphere. The solution was then cannula-transferred into 8 mm glass tubes, carefully layered with hexanes, and the tubes were flame sealed. X-ray quality crystals of [Fe(TPP)(CO)(1-MeIm)]·C$_6$H$_6$ were isolated after 25 days at 25 °C. IR $\nu_{CO}$ in KBr: 1968 cm$^{-1}$.

**X-Ray Crystallographic Studies.** All crystals were placed in inert oil, mounted on a glass pin, and transferred to the cold gas stream of the diffractometer. Crystal data were collected and integrated using a Bruker Apex system, with graphite monochromated Mo Kα ($\lambda$ = 0.71073 Å) radiation at 100 K (700 Series Oxford Cryostream) for all complexes. All data were collected to $2\theta_{max} \geq 65°$ with the exception of [Fe(TPP)(CO)(1,2-Me$_2$Im)] ($2\theta_{max}$ = 56.5°). The program SADABS[42] was applied for absorption corrections.

The structures of [Fe(TPP)(CO)(1-MeIm)]·C$_6$H$_6$ and [Fe(TPP)(CO)(1,2-Me$_2$Im)] were solved by direct methods in SHELXS-97,[43] while the structures of [Fe(TPP)(CO)(1,2-Me$_2$Im)]·C$_7$H$_8$ and [Fe(TPP)(CO)(2-MeHIm)]·C$_7$H$_8$ were solved using the Patterson method in SHELXS-97.[44] All structures were refined using SHELXL-97.[45] All nonsolvent atoms were found after successive full-matrix least-squares refinement cycles on $F^2$ and refined with anisotropic thermal parameters. Solvent molecule atoms were refined anisotropically when possible. Hydrogen atom positions were idealized with a riding model and fixed thermal parameters [$U_{ij} = 1.2U_{ij(eq)}$ or $1.5U_{ij(eq)}$] for the atom to which they are bonded with the exception of N−H hydrogen in [Fe(TPP)(CO)(2-MeHIm)]·C$_7$H$_8$ and the hydrogens of the 2-methyl group in [Fe(TPP)(CO)(1,2-Me$_2$Im)]·C$_7$H$_8$. These four hydrogen atoms were found in difference Fourier maps, and their positions and temperature factors were refined in successive full-matrix least-squares refinements.

Complete crystallographic details are given in the Supporting Information and are summarized in Table S1. The required 2-fold symmetry imposed on [Fe(TPP)(CO)(1,2-Me$_2$Im)] leads to a linear Fe−C−O bond angle and two separate orientations (equally occupied) of the 1,2-dimethylimidazole described with the Fe−N$_{Im}$ bond tilted off the 2-fold axis. A rigid group approximation was used to fully resolve the two distinct orientations of the ring. The rigid group orthogonal coordinates can be found in Table S26 in the Supporting Information. [Fe(TPP)(CO)(1,2-Me$_2$Im)]·C$_7$H$_8$ also contains a disordered 1,2-dimethylimidazole over two positions. These were refined as two rigid imidazole rings, which were found to have relative occupancies of 62%

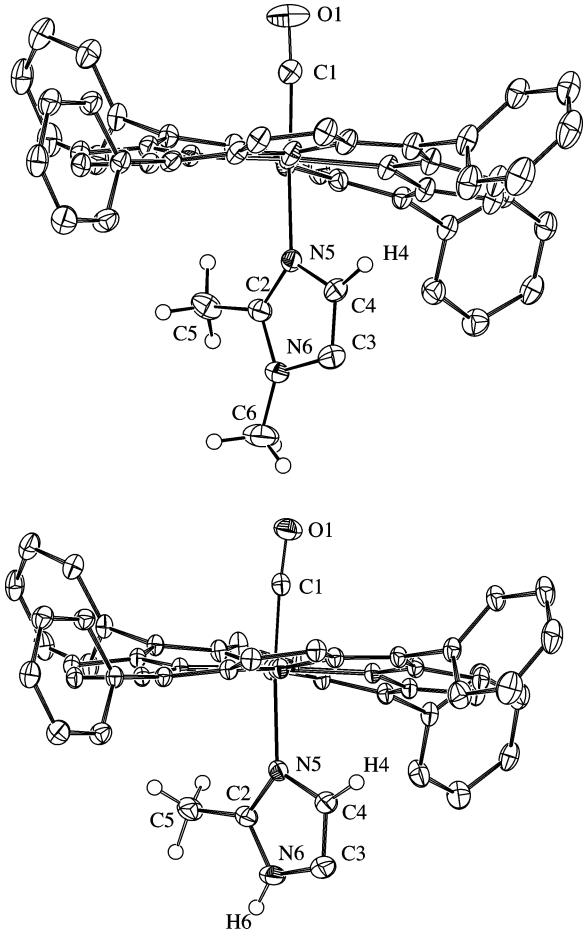


***Figure 1.*** ORTEP diagrams (50% probability ellipsoids) of (top) [Fe(TPP)(CO)(1,2-$Me_2$Im)]·$C_7H_8$ (only the major orientation of imidazole shown) and (bottom) [Fe(TPP)(CO)(2-MeHIm)]·$C_7H_8$. Significant hydrogen atoms are displayed, all other hydrogen atoms are omitted for clarity. Note the tilt of Fe−$N_{Im}$ off the heme normal and the near linearity of the Fe−C−O group.

for the major position and 38% for the minor position and unequal axial Fe−N distances.[46]

## Results

The crystal and molecular structures of four six-coordinate CO iron(II) porphyrinates have been obtained. The structures of [Fe(TPP)(CO)(1,2-$Me_2$Im)], [Fe(TPP)(CO)(1,2-$Me_2$Im)]·$C_7H_8$, and [Fe(TPP)(CO)(2-MeHIm)]·$C_7H_8$, all with sterically hindered imidazoles, have not previously been reported. We also report the structure of a benzene-solvated form of [Fe(TPP)(CO)(1-MeIm)] that has been previously isolated as a toluene solvate.[47,48]

Crystallographic details for all four structures are summarized in Table S1. ORTEP diagrams of [Fe(TPP)(CO)(1,2-$Me_2$Im)]·$C_7H_8$ and [Fe(TPP)(CO)(2-MeHIm)]·$C_7H_8$ are illustrated in Figure 1. The side-on view of these porphyrinates give a distinct perspective of not only the porphyrin core conformation but also the tilting of the Fe−$N_{Im}$ bond off the heme normal. The dihedral angles between the 24-atom porphyrin plane and the imidazole plane is 85° (for both orientations) and 82°, respectively. The ORTEP diagram for [Fe(TPP)(CO)(1,2-$Me_2$Im)] is shown in Figure 2. The side-on view illustrates the linear Fe−C−O group and symmetric disorder of the axial ligand that is required by crystallographically imposed 2-fold symmetry. The

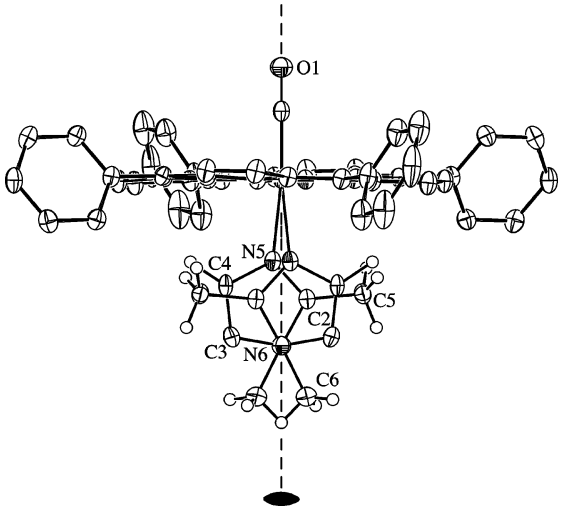


***Figure 2.*** ORTEP diagram (50% probability ellipsoids) of [Fe(TPP)(CO)(1,2-$Me_2$Im)]. Significant hydrogen atoms are displayed, all other hydrogen atoms are omitted for clarity. This diagram illustrates the linearity of the Fe−C−O group imposed by the 2-fold symmetry. The 2-fold disordered 1,2-$Me_2$Im ligand is shown.

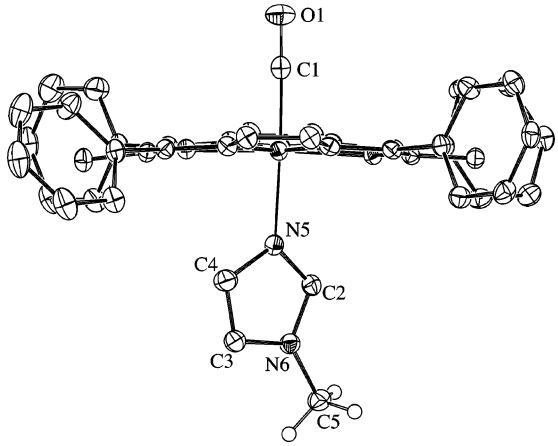


***Figure 3.*** ORTEP diagram (50% probability ellipsoids) of [Fe(TPP)(CO)(1-MeIm)]·$C_6H_6$. Significant hydrogen atoms are displayed, all other hydrogen atoms are omitted for clarity.

dihedral angle between the 24-atom plane of the porphyrin and the plane of the imidazole is 90° (symmetry imposed). The ORTEP diagram for [Fe(TPP)(CO)(1-MeIm)]·$C_6H_6$ is shown in Figure 3. This diagram illustrates the near linearity of the Fe−C−O and C−Fe−$N_{Im}$ angles. The dihedral angle between the 24-atom plane of the porphyrin and the plane of the imidazole is 83°.

Formal diagrams of atom displacements from the 24-atom mean planes of [Fe(TPP)(CO)(1,2-$Me_2$Im)]·$C_7H_8$ and [Fe(TPP)(CO)(2-MeHIm)]·$C_7H_8$ are given in Figure S1. In these and subsequent formal diagrams, the position of the imidazole methyl group at the 2-carbon position is indicated by the small circle, and the average Fe−$N_{pyrrole}$ distances are displayed. The relative orientation of the axial imidazole ligand is shown as a projection onto the core. Positive displacements are toward the CO. The angle between the imidazole plane and the nearest $N_p$−Fe−$N_p$ for [Fe(TPP)(CO)(1,2-$Me_2$Im)]·$C_7H_8$ and [Fe(TPP)(CO)(2-MeHIm)]·$C_7H_8$ is approximately 45°. The two imidazole orientations are also shown.

Formal diagrams of [Fe(TPP)(CO)(1-MeIm)]·$C_6H_6$ and [Fe(TPP)(CO)(1,2-$Me_2$Im)] showing atom displacements from the

***Scheme 1***

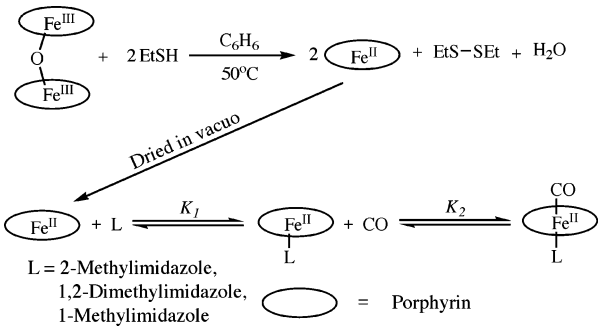


24-atom mean plane are illustrated in Figure S3 and Figure S2, respectively. The formal diagrams illustrate the angle between the imidazole plane and the nearest $N_p-Fe-N_p$ for both of these structures is approximately 30°. The two equally occupied imidazole orientations can also be observed.

Carbonyl stretching frequencies and notable structural features for these and related structures have been investigated. The $\nu_{C-O}$'s reported for the four new structures vary from 1968 to 1926 $cm^{-1}$. Mössbauer spectra were collected at 15−300 K in zero field for [Fe(TPP)(CO)(1,2-$Me_2$Im)]·$C_7H_8$ and [Fe(TPP)-(CO)(1-MeIm)]·$C_6H_6$.

## Discussion

**Synthetic Aspects.** The synthetic steps in preparing six-coordinate carbonyl iron(II) porphyrins are illustrated in Scheme 1. All reactions must be carried out under strict anaerobic conditions. While the synthesis of carbonyl iron(II) porphyrin complexes with unhindered imidazoles is straightforward, the synthesis of iron(II) carbonyl porphyrinates with hindered imidazoles is surprisingly difficult due to their reduced affinity for CO. Although the values of $K_1$, as illustrated in Scheme 1, for hindered and unhindered imidazoles are nearly equal, the CO binding constants ($K_2$) are substantially different.[16] Rougee and Brault report a 200-fold decrease in the CO binding constant when the trans ligand is a hindered imidazole compared to unhindered imidazole. This binding constant difference is such that rapid crystallization of carbonyl products yields a mixture. Thus, both the six-coordinate CO-ligated derivative and the five-coordinate imidazole-ligated species cocrystallize when the trans ligand is a hindered imidazole. This is not the case with unhindered imidazole derivatives. Thus, the isolation of the pure hindered imidazole derivatives, [Fe(TPP)(CO)(L)], is possible only by preparing and harvesting single crystals.

**Molecular Structures.** We report the molecular structures of four six-coordinate iron(II) carbonyl complexes determined at high resolution and high accuracy that allow us to make strong structural and spectroscopic correlations. These correlations will be given in subsequent sections.

Bond lengths and angles with uncertainties for the $L_{Im}-Fe-C-O$ coordination group for these four new structures and, for comparison, all known heme carbonyl structures are given in Table 1. The Fe−C−O angle in these new derivatives deviate only slightly from precise linearity. Values for [Fe(TPP)(CO)-(1,2-$Me_2$Im)]·$C_7H_8$, [Fe(TPP)(CO)(2-MeHIm)]·$C_7H_8$, and [Fe-(TPP)(CO)(1-MeIm)]·$C_6H_6$ are 175.9°, 176.0°, and 177.0°, respectively, while that for [Fe(TPP)(CO)(1,2-$Me_2$Im)] is 180°, as required by the imposed 2-fold axis. The Fe−C−O tilt for [Fe(TPP)(1,2-$Me_2$Im)], [Fe(TPP)(CO)(1,2-$Me_2$Im)], [Fe(TPP)-(CO)(2-MeHIm)]·$C_7H_8$, and [Fe(TPP)(CO)(1-MeIm)]·$C_6H_6$, defined as the angle between the Fe−C vector and the heme normal, are 0°, 4.2°, 1.1°, and 1.0°, respectively.

The presence of the hindering α-methyl group in the 2-methyl- or 1,2-dimethyl-substituted imidazoles leads to a modest off-axis tilt of the Fe−N bond from the heme plane normal. Values are 6.2° for [Fe(TPP)(CO)(1,2-$Me_2$Im)], 7.5° and 7.6° for [Fe(TPP)(CO)(1,2-$Me_2$Im)]·$C_7H_8$, 3.7° for [Fe-(TPP)(CO)(2-MeHIm)]·$C_7H_8$, and 3.4° for [Fe(TPP)(CO)-(1-MeIm)]·$C_6H_6$. A larger effect is the unequal Fe−N−C angles; the Fe−N−C angles for the carbon bearing the methyl group are ∼10.5° larger than that of the unsubstituted carbon (132.3°; (average) compared to 121.8°). This pattern is common to all known iron derivatives coordinated to hindered imidazoles.[65,66] Interestingly, the relative orientations of the two axial tilts are such that the axial $N_{Im}-Fe-C$ angles have values close to 180°. The hindered imidazole ligand also leads to some elongation of the $Fe-N_{Im}$ bond compared to analogous derivatives with unhindered imidazoles. There appears to be some variation in this axial bond length even with the same ligand, consequently we can only estimate the elongation effect as ≥∼0.04 Å.

However, the Fe−N bond distances trans to Fe−C(CO) are relatively long in all of the carbonyl complexes. The Fe−N(1-MeIm) distances are found to be ∼2.04 Å for the [Fe(Por)-(CO)(1-MeIm)] complexes (Table 1), and the analogous distance for derivatives with hindered imidazoles longer still. Estimates of the magnitude of the increase in Fe−N(L) can be determined by comparison with a series of bis-ligated six-coordinate iron-(II) porphyrinate complexes bonded to imidazole ligands.[67] The bis-imidazole complexes[67] display axial Fe−N(L) bonds ranging from 2.004(2) to 2.017(4) Å; a lengthening of ≥∼0.03 Å is thus inferred. The bond-lengthening is somewhat smaller than that observed for the thiocarbonyliron(II) porphyrinates where a lengthening of about 0.10 Å was inferred[68] or that in iron(II) nitrosyl porphyrinates where the Fe−N(L) distances of the ligand trans to nitrosyl is lengthened by >0.2 Å.[69−71] The carbonyl ligand thus has a significant structural trans effect, but one that is smaller than those seen in a number of other diatomic ligands coordinated to iron(II) porphyrinates.

The four molecules whose structures are reported here all have nonplanar porphyrin core conformations. Detailed formal diagrams of the displacements of each atom from the mean plane of the 24-atom core are displayed in Figures S1−S3 of the Supporting Information.

The toluene solvates of [Fe(TPP)(CO)(1,2-$Me_2$Im)] and [Fe-(TPP)(CO)(2-MeHIm)] have nearly identical (ruffled) core conformations, as can be seen in Figure S1. Indeed, crystals of the two molecules are isomorphous and the molecular structures are nearly indistinguishable with the exception of small differences in the axial ligands. This is shown in the overlay diagram of Figure 4. The overlay diagram was constructed as described in the figure caption. The largest difference is in the position of the CO oxygen atoms that are 0.384 Å apart.

The ruffled cores in [Fe(TPP)(CO)(1,2-$Me_2$Im)]·$C_7H_8$ and [Fe(TPP)(CO)(2-MeHIm)]·$C_7H_8$ are the result of the imidazole orientation. The projection of the imidazole plane on the porphyrin core is approximately 45° from the nearest $Fe-N_p$

(70) Scheidt, W. R.; Brinegar, A. C.; Ferro, E. B.; Kirner, J. F. *J. Am. Chem. Soc.* **1977**, *99*, 7315.
(71) Wyllie, G. R. A.; Schulz, C. E.; Scheidt, W. R. *Inorg. Chem.* **2003**, *42*, 5722.

***Table 1.*** Carbonyl Stretching Frequencies and Notable Structural Features for [Fe(TPP)(CO)(1,2-$Me_2$Im)]·$C_7H_8$, [Fe(TPP)(CO)(2-MeHIm)]·$C_7H_8$, [Fe(TPP)(CO)(1,2-$Me_2$Im)], and [Fe(TPP)(CO)(1-MeIm)]·$C_6H_6$ and Related Compounds

| | Fe–C[a] | Fe–C–O[b] | Fe–$L_{ax}$[a] | C–Fe–$L_{ax}$[b] | C–O[a] | $\nu_{C-O}$[c] | $\nu_{C-O}$[c] | ref |
|---|---|---|---|---|---|---|---|---|
| **[Fe(TPP)(CO)(2-MeHIm)]·$C_7H_8$** | **1.7410(14)** | **175.96(13)** | **2.1018(12)** | **175.42(5)** | **1.1488(17)** | **1926[d]** | | **tw** |
| **[Fe(TPP)(CO)(2-MeHIm)]** | | | | | | | **1972[e]** | **tw** |
| **[Fe(TPP)(CO)(1,2-$Me_2$Im)]·$C_7H_8$** | **1.7537(15)** | **175.95(14)** | **2.0779(11)** | **176.77(6)** | **1.1408(19)** | **1948, 1953[d]** | | **tw** |
| **[Fe(TPP)(CO)(1,2-$Me_2$Im)]·$C_7H_8$[f]** | | | **2.1402(18)** | **168.73(8)** | | **1948, 1953[d]** | | **tw** |
| **[Fe(TPP)(CO)(1,2-$Me_2$Im)]** | **1.764(2)** | **180[g]** | **2.133(2)** | **173.85(9)** | **1.138(3)** | **1963[d]** | | **tw** |
| **[Fe(TPP)(CO)(1,2-$Me_2$Im)]** | | | | | | | **1972[e]** | **54, tw** |
| **[Fe(TPP)(CO)(1-MeIm)]·$C_6H_6$** | **1.7600(17)** | **177.03(15)** | **2.0503(14)** | **176.78(6)** | **1.139(2)** | **1968[d]** | | **tw** |
| [Fe(TPP)(CO)(1-MeIm)]·$C_7H_8$ | 1.793(3) | 179.3(3) | 2.071(2) | 178.3(3) | 1.061(3) | | 1969[h] | 47 |
| [Fe(TPP)(CO)(1-MeIm)]·2.5$C_7H_8$ | 1.7636(13) | 178.76(13) | 2.0400(11) | 178.38(5) | 1.1437(17) | 1967[d] | | 48 |
| **[Fe(TPP)(CO)(1-MeIm)]** | | | | | | | **1969[i]** | **tw** |
| [Fe($C_2$Cap)(CO)(1-MeIm)] | 1.742(7) | 172.9(6) | 2.043(6) | 174.7(3) | 1.161(8) | 2000[d] | | 52 |
| [Fe($C_2$Cap)(CO)(1-MeIm)] | 1.748(7) | 175.9(6) | 2.041(5) | 177.8(3) | 1.158(8) | 2000[d] | | 52 |
| [Fe($OC_3$OPor)(CO)(1-MeIm)]·1.5$C_7H_8$ | 1.748(7) | 173.9(7) | 2.027(5) | 174.5(3) | 1.171(8) | 1978[d] | | 53 |
| [Fe($OC_3$OPor)(CO)(1,2-$Me_2$Im)]·2$CHCl_3$ | 1.713(8) | 180[g] | 2.102(6) | 173.0(2) | 1.161(10) | 1974[d] | | 53 |
| [Fe($Tpiv_2C_{12}$P)(CO)(1-MeIm)] | 1.728(6) | 180[g] | 2.062(5) | 180[g] | 1.149(6) | | 1958[i] | 55 |
| [Fe(TpivPP)(CO)(1-MeIm)] | | | | | | | 1965[i] | 56, 19 |
| [Fe(OEP)(CO)(1-MeIm)] | 1.744(5) | 175.1(4) | 2.077(3) | 176.8(2) | 1.158(5) | | 1965[h] | 57 |
| [Fe($C_3$Cap)(CO)(1,2-$Me_2$Im)] | 1.800(13) | 178.0(13) | 2.046(10) | 178.9(5) | 1.107(13) | | 1984[e] | 58 |
| [Fe($C_3$Cap)(CO)(1,2-$Me_2$Im)] | | | | | | | 1984[j] | 54 |
| [Fe($C_2$Cap)(CO)(1,2-$Me_2$Im)] | | | | | | | 1999[j] | 54 |
| [Fe(β-PocPivP)(CO)(1,2-$Me_2$Im)] | 1.768(7) | 172.5(6) | 2.079(5) | 176.3(3) | 1.148(7) | | | 59 |
| [Fe(TPP)(CO)(Py)] | 1.77(2) | 179(2) | 2.10(1) | 177.5(8) | 1.12(2) | | 1980[k] | 60 |
| [Fe(OEP)(CO)(Py)] | | | | | | | 1967 | 61 |
| [Fe(Deut)(CO)(THF)] | 1.706(5) | 178.3(14) | 2.127(4) | 177.4(9) | 1.144(5) | | 1955[l] | 62 |
| [Fe(TPP)(CO)(THF)] | | | | | | | 1955[k] | 62 |
| [Fe(TpivPP)(CO)(THF)] | | | | | | | 1961[k] | 63 |
| [Fe(TPP)(CO)(SEt)] | 1.78(1) | | 2.352(2) | | 1.17(1) | | 1920[m] | 64 |
| [Fe(TpivPP)(CO)(THT)] | | | | | | | 1970[i] | 63 |
| HbCO | | | | | | | 1951[n] | 13 |
| MbCO | | | | | | | 1927[n] | 34 |
| | | | | | | | 1945[n] | 34 |
| | | | | | | | 1969[n] | 34 |

[a] Å. [b] deg. [c] $cm^{-1}$. [d] Nujol mull. [e] Toluene solution saturated with base. [f] Second conformation of the 1,2-$Me_2$Im is approximately 38% occupied. [g] Symmetry imposed linearity. [h] $CDCl_2$ solution. [i] Benzene solution. [j] Toluene solution. [k] Pyridine solution. [l] Tetrahydrofuran solution. [m] Chlorobenzene solution. [n] Aqueous solution.

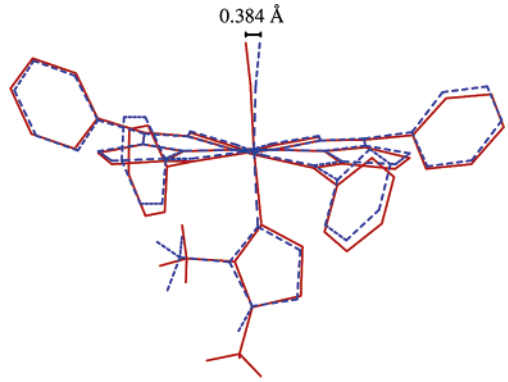


***Figure 4.*** An overlay diagram showing the structures of [Fe(TPP)(CO)(1,2-$Me_2$Im)]·$C_7H_8$ (−) and [Fe(TPP)(CO)(2-MeHIm)]·$C_7H_8$ (− − −). These structures were fit by superimposing the four pyrrole nitrogens and orientated so the mean plane of these nitrogens are perpendicular to the page. The molecules can be seen to have nearly identical core and phenyl ring conformations. The CO oxygens are separated by 0.384 Å.

bond (Figure S1). This places the 2-methylimidazole group near a methine carbon atom, and the steric congestion leads to core ruffling. The effect of the two different hindered imidazoles on core conformations is nearly identical. Some time ago, Hoard[72,73] pointed out that such core ruffling leads to a shortening of the equatorial Fe−$N_p$ bonds. [Fe(TPP)(CO)(1,2-$Me_2$Im)]·$C_7H_8$ and [Fe(TPP)(CO)(2-MeHIm)]·$C_7H_8$ have average Fe−$N_p$ bond lengths of 1.985(8) and 1.988(6) Å, and the shortening observed for these two derivatives is in general agreement with expectations. Ruffled-core conformations have been observed for a number of six-coordinate iron(II) porphyrinates with a single diatomic ligand. Ruffled cores (Fe−$N_p$ distances given in parentheses) have been observed in [Fe(Deut)(CO)(THF)] (1.981(3) Å),[62] [Fe(TpivPP)($O_2$)(1-MeIm)] (1.979(13) Å),[74] [Fe(TpivPP)($O_2$)(2-MeHIm)] (1.995(4) Å),[75] [Fe(OEP)(CS)($CH_3$OH)] (1.993(1) Å),[68] and [Fe(TpivPP)(CO)($NO_2$)]$^-$ (1.997(6) Å).[76]

The other two derivatives, [Fe(TPP)(CO)(1-MeIm)]·$C_6H_6$ and [Fe(TPP)(CO)(1,2-$Me_2$Im)], have core conformations that are primarily saddled and are similar to each other. These two complexes contain imidazoles that are oriented approximately 30° from the nearest Fe−$N_p$ bond (see Figures S2 and S3.) The average Fe−$N_p$ bond distance for [Fe(TPP)(CO)(1-MeIm)]·$C_6H_6$ and [Fe(TPP)(CO)(1,2-$Me_2$Im)] are 2.005(6) and 2.004(1) Å, respectively, somewhat longer than those observed for the ruffled derivatives.

Saddling is a commonly observed core conformation of six-coordinate iron(II) porphyrinates with a single diatomic ligand. Saddled cores (Fe−$N_p$ distances given in parentheses) have been observed in [Fe(OEP)(CO)(1-MeIm)] (2.000(3) Å),[57] [Fe(TPP)(CO)(Py)] (2.02(3) Å),[60] [Fe(TPP)(NO)(1-MeIm)] (2.009(13)

(72) Hoard, J. L. *Ann. N. Y. Acad. Sci.* **1973**, *206*, 18.
(73) Collins, D. M.; Scheidt, W. R.; Hoard, J. L. *J. Am. Chem. Soc.* **1972**, *94*, 6689.
(74) Jameson, G. B.; Rodley, G. A.; Robinson, W. T.; Gagne, R. R.; Reed, C. A.; Collman, J. A. *Inorg. Chem.* **1978**, *17*, 850.
(75) Jameson, G. B.; Molinaro, F. S.; Ibers, J. A.; Collman, J. P.; Brauman, J. I.; Rose, E.; Suslick, K. S. *J. Am. Chem. Soc.* **1980**, *102*, 3224.
(76) Nasri, H.; Ellison, M. K.; Shang, M.; Schulz, C. E.; Scheidt, W. R. *Inorg. Chem.* **2004**, *43*, 2932.

***Table 2.*** Mössbauer Data for [Fe(TPP)(CO)(L)] and Related Complexes

| complex[a] | temp, K | $\Delta E_q$[b] | $\delta$[b] | ref |
|---|---|---|---|---|
| [Fe(Por)(CO)(L)] | | | | |
| [Fe(TPP)(CO)(1,2-$Me_2$Im)]$C_7H_8$ | 293 | 0.71 | 0.17 | tw |
| | 200 | 0.65 | 0.23 | tw |
| | 100 | 0.66 | 0.29 | tw |
| | 15 | 0.64 | 0.25 | tw |
| [Fe(TPP)(CO)(1-MeIm)]$C_6H_6$ | 293 | 0.35 | 0.16 | tw |
| | 200 | 0.32 | 0.24 | tw |
| | 100 | 0.32 | 0.25 | tw |
| | 15 | 0.30 | 0.26 | tw |
| [Fe(OEP)(CO)(1-MeIm)]$C_6H_6$ | 293 | 0.40 | 0.18 | tw |
| | 200 | 0.37 | 0.25 | tw |
| | 100 | 0.37 | 0.23 | tw |
| | 15 | 0.34 | 0.24 | tw |
| [Fe(TPP)(CO)(1-MeIm)] | 77 | 0.35 | 0.20 | 80 |
| [Fe(TPP)(CO)(Py)] | 77 | 0.57 | 0.28 | 80 |
| [Fe(TPP)(CO)(Pip)] | 295 | 0.53 | 0.18 | 81 |
| MbCO | 4.2 | +0.35 | 0.27 | 82 |
| HbCO | 4.2 | +0.36 | 0.26 | 83 |
| [Fe(Por)(CS)(L)] and [Fe(Por)(CS)] | | | | |
| [Fe(OEP)(CS)(1-MeIm)] | 293 | 0.47 | 0.03 | 68 |
| | 4.2 | 0.42 | 0.14 | 68 |
| [Fe(OEP)(CS)] | 293 | 1.95 | −0.03 | 68 |
| | 4.2 | 1.93 | 0.08 | 68 |
| [Fe(Por)(NO)(L)] and [Fe(Por)(NO)] | | | | |
| [Fe(TPP)(NO)(1-MeIm)] | 293 | 0.80 | 0.24 | 71 |
| | 4.2 | 0.73 | 0.35 | 71 |
| [Fe(TPP)(NO)] | 4.2 | 1.24 | 0.35 | 84 |
| [Fe(OEP)(NO)] | 100 | 1.26 | 0.35 | 85 |

[a] Abbreviations given in the references. [b] Value in mm/s.

Å),[71] [Fe(TPP)(NO)($NMe_2$Py)] (2.006(11) Å),[71] [Fe(TPP)(NO)-(4-MePip)] (2.009(8) Å),[71] [Fe(OEP)(CS)(1-MeIm)] (2.001(4) Å),[68] and [Fe(OEP)(CS)(Py)] (1.999(1) Å).[68]

The relationship between core conformation and the orientation of planar axial ligands is clearly shown in these newly reported species. [Fe(TPP)(CO)(1,2-$Me_2$Im)]·$C_7H_8$ and [Fe-(TPP)(CO)(1,2-$Me_2$Im)] (with a 2-fold symmetry axis along the Fe−C−O) have identical ligands, yet their imidazole orientations are substantially different and subsequently so are their core conformations. Although the energies associated with the crystallization of the two crystalline forms is not well understood, it is interesting to note that the crystal system formed over the shorter time is the slightly more ordered. These two sets of molecular structures further illustrate that axial ligand orientations affect core conformations. Finally, we note that there continues to be speculation that core perturbations may play a crucial role in the activity of heme centers in biology.[77−79]

**Mössbauer.** Variable-temperature Mössbauer data for three new carbonyl derivatives, two of which have been structurally characterized, have been obtained. These new data are reported in Table 2 along with previously reported data from the literature. The data are consistent with other low-spin carbonyls. The new derivatives display very little temperature dependence on either the quadrupole splitting or the isomer shift value in the temperature range of 15−293 K. The quadrupole splitting value for [Fe(TPP)(CO)(1,2-$Me_2$Im)]·$C_7H_8$ with its sterically hindered imidazole ligand has a higher value than that of any other derivative. This suggests that the magnitude of the quadrupole splitting could be sensitive to variation in the geometry around the iron atom. A systematic investigation of this issue is currently being planned.

**Environmental Effects on $\nu_{C-O}$ Values.** In heme proteins, CO stretching frequencies have been found to vary from 1904 to 1984 $cm^{-1}$.[86] These differences in $\nu_{C-O}$ are believed to be the result of both the interactions with specific residues in the ligand binding pocket and generalized electrostatic effects. In early IR studies, the CO stretching frequencies of MbCO were found to vary between 1927 and 1969 $cm^{-1}$. These were perhaps the first studies that demonstrated that the protein environment had a substantial effect on CO stretching frequencies.[87] The multiple CO stretching frequencies are believed to reflect differences in ligand binding pocket conformational states.[34−36] The relative intensities of these modes are affected by pH, temperature, and pressure.[88] Three CO stretching frequencies are found in MbCO. These states and CO frequencies are 1969 ($A_0$), 1945 ($A_1$), and 1927 $cm^{-1}$ ($A_3$).[35] Subsequently, CO has been utilized to examine the electrostatic properties near the diatomic binding pocket in Mb and Mb mutants. Phillips et al. have demonstrated that the stretching frequency of CO can act as a gauge of the electrostatic fields near the ligand binding site.[14] Thus, the vibrational properties of CO gives a useful experimental measure of environmental effects in heme proteins. Understanding such effects could assist in determining how discrimination in binding between NO, CO, and $O_2$ in heme proteins arises.[14,23] In an interesting theoretical study, Franzen suggests that specific orientations of the ligand binding pocket groups play an important role in the CO/$O_2$ discrimination.[89]

The four iron(II) carbonyl derivatives reported here show a large range of CO stretching frequencies in the solid state. The CO absorbances, measured on carefully mulled single crystals, showed $\nu_{C-O}$'s from 1968 to 1926 $cm^{-1}$. These values show a larger-than-expected range of frequencies, since the generally observed value for $\nu_{C-O}$ for "classical" [Fe(Por)(CO)(L)] derivatives is ∼1970 $cm^{-1}$.[61] Indeed, the CO stretching frequencies of these four complexes *in toluene solution* are all observed at 1969−1972 $cm^{-1}$. We expect that the complexes have a

(77) (a) Ma, J. G.; Zhang, J.; Franco, R.; Jia, S. L.; Moura, I.; Moura, J. J.; Kroneck, P. M.; Shelnutt, J. A. *Biochemistry* **1998**, *37*, 12431. (b) Senge, M. O. In *The Porphyrin Handbook*; Kadish, K. M., Smith, K. M., Guilard, R., Eds.; Academic Press: San Diego, 2000; Vol. 1, p 240. (c) Kadish, K. M.; Van Camelbecke, E.: Royal, G. In *The Porphyrin Handbook*; Kadish, K. M., Smith, K. M., Guilard, R., Eds.; Academic Press: San Diego, 2000; Vol. 8, p 3.
(78) Roberts, S. A.: Weichsel, A.; Qiu, Y.; Shelnutt, J. A.; Walker, F. A.; Montfort, W. R. *Biochemistry* **2001**, *40*, 11327.
(79) Pellicena, P.; Karow, D. S.; Boon, E. M.; Marletta, M. A.; Kuriyan, J. *Proc. Natl. Acad. Sci. U.S.A.* **2004**, *101*, 12854.
(80) Havlin, R. H.; Godbout, N.; Salzmann, R.; Wojdelski, M.; Arnold, W.; Schulz, C. E. Oldfield, E. *J. Am. Chem. Soc.* **1998**, *120*, 3144.
(81) James, B. R.; Sams, J. R.; Tsin, T. B.; Reimer, K. J. *J. Chem. Soc., Chem. Commun.* **1978**, 746.
(82) Maeda, Y.; Harami, T.; Morita, Y.; Trautwein, A.; Gonser, U. *J. Chem. Phys.*, **1981**, *75*, 36.
(83) Lang, G.: Marshall, W. *Proc. Phys. Soc.*, **1981**, *75*, 36.
(84) Nasri, H.; Ellison, M. K.; Chen, S.; Hunyh, B. H.; Scheidt, W. R. *J. Am. Chem. Soc.* **1997**, *119*, 6274.
(85) Bohle, D. S.; Debrunner, P. G.; Fitzgerald. J.; Hansert, B.; Hung, C.-H.; Thompson, A. J. *J. Chem. Soc., Chem. Commun.* **1997**, 91.
(86) Vogel, K. M.; Kozlowski, P. M.; Zgierski, M. Z.; Spiro, T. G. *Inorg. Chim. Acta* **2000**, *297*, 11.
(87) McCoy, S.; Caughey, W. S. In *Probes of Structure and Function of Macromolecules and Membranes, Probes of Enzymes and Hemoproteins*; Chance, B., Yonetani, T., Mildvan, A. S., Eds.; Academic: New York, 1971; Vol. 2, p 289.
(88) Fuchsman, W. H.; Appleby, C. A. *Biochemistry* **1979**, *18*, 1309. Ansari, A.; Berendzen, J.; Braunstein, D.; Cowen, B. R.; Frauenfelder, H.; Hong, M. K.; Iben, I. E. T.; Johnson, B.; Ormos, P.; Sauke, T. B.; Scholl, R.; Schulte, A.; Steinbach, P. J.; Vittitow, J.; Young, R. D. *Biophys. Chem.* **1987**, *26*, 337. Frauenfelder, H.; Alberding, N. A.; Ansari, A.; Braunstein, D.; Cowen, B. R.; Hong, M. K.; Iben, I. E. T.; Johnson, J. B.; Luck, S.; Marden, M. C.; Mourant, J. R. *J. Phys. Chem.* **1990**, *94*, 1024.
(89) Franzen, S. *J. Am. Chem. Soc.* **2002**, *124*, 13271.

***Table 3.*** Listing of the Closest Contacts to CO (All H···O ≤ 3.5 Å) and Related Geometrical Features

| | [Fe(TPP)(CO)-(2-MeHIm)]·$C_7H_8$ | [Fe(TPP)(CO)-(1,2-$Me_2$Im)]·$C_7H_8$ (major)[a] | [Fe(TPP)(CO)-(1,2-$Me_2$Im)]·$C_7H_8$ (minor)[a] | [Fe(TPP)(CO)-(1,2-$Me_2$Im)] | [Fe(TPP)(CO)-(1-MeIm)]·$C_6H_6$ |
|---|---|---|---|---|---|
| $\nu_{C-O}$, $cm^{-1}$ | 1926 | 1953 | 1948 | 1963 | 1972 |
| O···H, (type)[b] | 2.38 (N−H[c]) | 2.53 ($CH_3$[d]) | 2.86 (ImC−H[e]) | 2.62 ($\beta$C−H[f]) | 2.65 (ImC−H) |
| O···X, Fe···O···X | 3.16, 114.7 | 2.96, 117.5 | 3.66, 96.2 | 3.26, 126.6 | 3.08, 143.4 |
| X−H···O | 166.7 | 106.7 | 139.3 | 125.2 | 108.2 |
| O···H, (type)[b] | 2.72 (Ph−H[g]) | 2.71 ($CH_3$) | 3.11 ($CH_3$) | 2.62 ($\beta$C−H) | 2.71 (Ph−H) |
| O···X, Fe···O···X | 3.38, 124.7 | 2.96, 79.8 | 3.68, 105.4 | 3.26, 126.6 | 3.14, 129.1 |
| X−H···O | 127.3 | 91.9 | 136.8 | 125.2 | 108.3 |
| O···H, (type)[b] | 3.11 (Ph−H) | 3.09 ($CH_3$) | 2.60 (Ph−H) | 2.79 (Ph−H) | 2.84 (Ph−H) |
| O···X, Fe···O···X | 3.56, 101.9 | 2.96, 101.0 | 3.29, 155.0 | 3.17, 104.0 | 3.33, 118.0 |
| X−H···O | 112.6 | 73.2 | 129.7 | 105.3 | 112.8 |
| O···H, (type)[b] | 3.09 ($CH_3$) | 2.60 (Ph−H) | 3.24 (Ph−H) | 2.79 (Ph−H) | 2.95 (Ph−H) |
| O···X, Fe···O···X | 3.91, 99.7 | 3.29, 155.0 | 3.61, 111.7 | 3.17, 104.0 | 3.26, 105.1 |
| X−H···O | 142.2 | 129.7 | 105.2 | 105.3 | 100.5 |
| O···H, (type)[b] | − | 3.24 (Ph−H) | − | 3.20 (Ph−H) | 2.98 ($CH_3$) |
| O···X, Fe···O···X | − | 3.61, 111.7 | − | 3.40, 103.9 | 3.30, 112.2 |
| X−H···O | − | 105.2 | − | 93.7 | 100.2 |
| O···H, (type)[b] | − | − | − | 3.20 (Ph−H) | 3.08 ($CH_3$) |
| O···X, Fe···O···X | − | − | − | 3.40, 103.9 | 3.30, 112.2 |
| X−H···O | − | − | − | 93.7 | 94.5 |

[a] Major orientation and minor orientation of the adjacent imidazole. [b] Each entry consists of three lines. Line 1 has the O···H distance in Å, followed by H-atom type. Line 2 has the O···X distance in Å, where X is the atom to which the H is bonded, followed by the Fe···O···X angle in degrees, followed by line 3 where the X−H···O angle in degrees is given. [c] Imidazole N−H. [d] Imidazole 2-methyl. [e] $\beta$-pyrrole H. [f] Imidazole 3-carbon H. [g] Phenyl H.

common environment in the toluene solution. The solution IR measurement for [Fe(TPP)(CO)(1-MeIm)] is straightforward, but the solution equilibria with the hindered imidazoles/CO requires measurements with a CO-saturated solution and high concentrations of the imidazole. When both of these conditions are satisfied, a single C−O stretching frequency is observed for a toluene solution of [Fe(TPP)(CO)(1,2-$Me_2$Im)]; similar results for [Fe(TPP)(CO)(2-MeHIm)] are observed with the band for the six-coordinate CO complexes clearly at 1972 $cm^{-1}$. The small range of *solution* CO stretching frequencies clearly indicates that the effect of the trans imidazole ligand is minimal. Thus, the available data strongly suggest that the decreased solid-state CO frequencies in these four CO derivatives are the result of solid-state environmental effects. Accordingly, we have examined the crystal structures and the CO environment of the four complexes in detail.

We first discuss the crystal structures of [Fe(TPP)(CO)(2-MeHIm)]·$C_7H_8$ and [Fe(TPP)(CO)(1,2-$Me_2$Im)]·$C_7H_8$ where the largest solid-state influence on $\nu_{C-O}$ is displayed. In these two isomorphous crystal structures, the molecules pack in the herringbone-like pattern shown in Figure S4. There are a number of O···H contacts less than 3.5 Å in all four derivatives (tabulated in Table 3); the closest contacts in these two derivatives come from contact with atoms of the coordinated imidazole of an adjacent molecule. The herringbone packing in the crystal structure of [Fe(TPP)(CO)(2-MeHIm)]·$C_7H_8$ places the N−H hydrogen from the adjacent imidazole at the proper distance and orientation for a hydrogen-bonding interaction. The O···H and O···N distances are 2.38 and 3.16 Å, respectively. The Fe···O···H angle of [Fe(TPP)(CO)(2-MeHIm)]·$C_7H_8$ is 112.0°, and the Fe···O···N angle is 114.7°. The canonical hydrogen bond contact distances for O···H and O···N are 2.0 and 2.9 Å, respectively.[90] Although the observed O···H distance of 2.38 Å is not the shortest possible such distance, shorter O···H distances typically involve an oxygen with a negative charge. However, the distance is clearly consistent with a real hydrogen-bonding interaction. This interaction of the neighboring imidazole N−H hydrogen with the carbonyl oxygen leads to a 46 $cm^{-1}$ shift from the solution IR measurement to 1926 $cm^{-1}$ in the solid state. This low frequency is reminiscent of the 1927 $cm^{-1}$ frequency observed for the $A_3$ conformer of sperm whale Mb,[35] that has been attributed to hydrogen bonding from the distal histidine (H64).[30,32,34]

The [Fe(TPP)(CO)(1,2-$Me_2$Im)]·$C_7H_8$ crystal lattice places methyl hydrogen atoms from the closest neighboring coordinated imidazole close to the carbonyl oxygen atom. The crystalline disorder described earlier leads to two distinct environments for the carbonyl oxygen atom from the two orientations of the coordinated imidazole, as shown in Figure 5. For the major ligand orientation, the O···H and O···C distances are 2.50 and 2.98 Å, respectively. The major orientation also has a second hydrogen from the methyl group with an O···H distance of 2.69 Å. The Fe···O···H angle of [Fe(TPP)(CO)(1,2-$Me_2$Im)]·$C_7H_8$ is 118.5° and the Fe···O···C angle is 101.0°. The minor orientation O···H and O···C distances from the imidazole methyl group are 3.11 and 3.68 Å, respectively. Indeed the closest contacts in the minor orientation are those in common with those of the major orientation (see Table 3). If the close methyl group environment is influencing $\nu_{C-O}$, two CO bands would be expected in the solid state. Indeed, there are two bands; the split in the $\nu_{C-O}$ band shown in Figure 6. Consistent with the unequal occupation of the two imidazole sites, the intensities of the two bands are not equal. The major orientation, at 62% occupancy, likely accounts for the more intense absorbance at 1953 $cm^{-1}$, while the minor orientation, at 38% occupancy, has $\nu_{C-O}$ at 1948 $cm^{-1}$. Thus, the two frequencies represent the difference in moving the methyl group about 0.7 Å closer to the carbonyl oxygen, as seen in Figure 5. That there are two $\nu_{C-O}$ values clearly shows that a methyl group close to the CO oxygen has an effect; that the effect of a closer methyl group approach apparently leads to a higher value of the stretching frequency is perhaps unexpected. However, single-site mutations

(90) Hamilton, W. C.; Ibers, J. A. In *Hydrogen Bonding in Solids*; Benjamin, W. A.: New York, 1968; p 16.

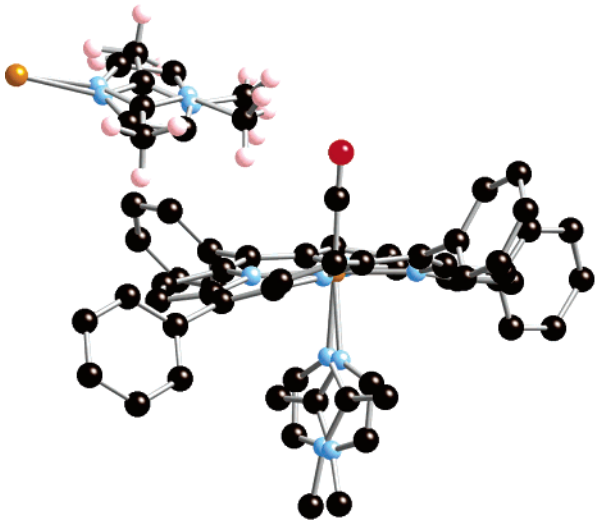

***Figure 5.*** Diagram illustrating the approach of methyl group hydrogens from the two distinct ligand orientations to the C−O of an adjacent molecule in [Fe(TPP)(CO)(1,2-$Me_2$Im)]·$C_7H_8$. The major 1,2-dimethylimidazole orientation has H···OC distances of 2.50 and 2.69 Å, and the C···OC distance is 2.96 Å. In the minor orientation, the C···OC distance has increased to 3.68 Å.

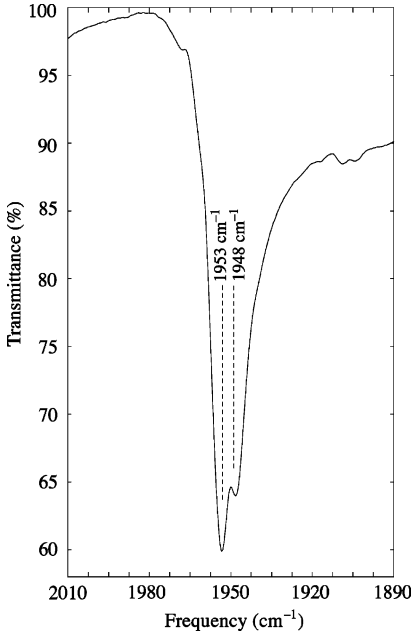


***Figure 6.*** IR spectrum of a single crystal of [Fe(TPP)(CO)(1,2-$Me_2$Im)]·$C_7H_8$ mulled in Nujol. Two C−O stretches are observed as a result of distinct methyl group interactions with two orientations of a 1,2-dimethylimidazole from an adjacent molecule in the crystal lattice.

in MbCO in which the distal histidine is changed to leucine, isoleucine, or valine are all observed to have $\nu_{C-O}$ increased from the $A_1$ value (native) of 1945 $cm^{-1}$.[14]

Interestingly, there is a small difference in the tilt of the carbonyl ligand in the two isomorphous species [Fe(TPP)(CO)(L)], L = 2-methyl- and 1,2-dimethylimidazole. This is shown by the difference (0.38 Å) in the oxygen atom position when the two cores are overlaid as shown in Figure 4. The differences are such that the N−H···O interaction appears to be attractive (CO tilts toward imidazole) while that of the $CH_3$···O interaction appears to be less attractive to modestly repulsive (CO tilts away from imidazole).

The unsolvated form of [Fe(TPP)(CO)(1,2-$Me_2$Im)] is packed into a lattice with all porphyrin planes parallel. The environment of the CO oxygen has a pair of (2-fold-equivalent) O···H and O···C separations of 2.62 and 3.26 Å, respectively; the Fe···O···H angles are 138.8°. The hydrogen atoms are from the $\beta$-carbons of adjacent porphyrins. Aspects of this environment are illustrated in Figure S7. This environment leads to $\nu_{C-O}$ = 1963 $cm^{-1}$, shifted from the 1972 $cm^{-1}$ observed in toluene solution. Even though the oxygen−hydrogen atom contacts are closer in this derivative than in the solvated form, the difference in the orientation and symmetry of the close contacts leads to a smaller shift in $\nu_{C-O}$ from the solution value.

The solid-state C−O stretching frequency in [Fe(TPP)(CO)(1-MeIm)]·$C_6H_6$ is unshifted from its solution value. Although the carbonyl oxygen contact distances in this solid-state species are not significantly different from those of other derivatives, the detailed geometry has some significant differences. The closest contact has the C−O bond nearly parallel to the H−C bond of the imidazole of an adjacent molecule; the contacts are relatively short at O···H and O···C distances of 2.651 and 3.082 Å, respectively. The unshifted value (1968 $cm^{-1}$) of $\nu_{C-O}$ clearly shows that short contact distances alone will not shift the vibration. The differences in the orientation of the adjacent imidazole in the three derivatives with close imidazole approaches are compared in Figure 7. The observed structural data and associated vibrational stretching frequencies for bound CO show that H-interactions with the CO oxygen atom that occur from the side will be much more significant than those that occur from the end. This generalization had been suggested by Franzen[89] on the basis of detailed ligand binding pocket modeling calculations.

These structural results clearly show that the effects of close contacts on $\nu_{C-O}$ in the carbonyl complexes depends on the distance, hydrogen-atom type, and orientation of the hydrogen-atom contacts to the CO oxygen atom. All variables are significant, and dissecting the individual contributions is clearly a challenge. Phillips et al.[37] have approached this from a study of the distal pocket electrostatic potential of wild type and Mb mutants. These studies have demonstrated that much of the $\nu_{C-O}$ shifts to higher frequencies are due to the loss of hydrogen-bonding interactions with histidine 64 (H64) in the distal binding pocket.[14] The calculations of Franzen,[89] as noted above, emphasize the importance of the orientation between the H-group and the oxygen atom in addition to the generalized electrostatic potential. Indeed, there are other possible contributions to the value of $\nu_{C-O}$ including the possibility of core conformation effects. It is important to note that the detailed structural information we have provided allows for the possibility of further detailed calculations.

Schlicting and co-workers have carried out a high-resolution (1.15 Å) structure determination of MbCO.[30] In this study, three different conformers that involve differing orientations of the distal histidine 64 were found and were associated with $\nu_{C-O}$ of conformers $A_1$, $A_3$, and $A_0$. Conformer $A_3$ (1927 $cm^{-1}$), which is a minor occupancy conformer, displays a hydrogen bond from the histidine N−H. Other investigators (Sage[91] and Ray et al.[92]) have suggested that $A_1$ (1945 $cm^{-1}$) is the most

(91) Sage, J. T. *JBIC* **1994**, *116*, 4139.
(92) Ray, G. B.; Li, X.-Y.; Ibers, J. A.; Sessler, J. L.; Spiro, T. G. *J. Am. Chem. Soc.* **1994**, *116*, 162.

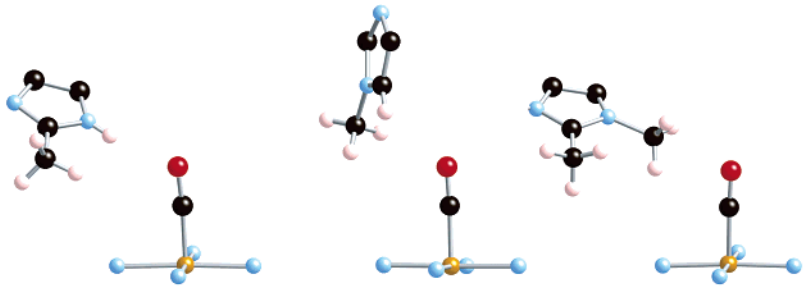

***Figure 7.*** Drawing comparing the orientation of the closely approaching imidazole ligand in [Fe(TPP)(CO)(2-MeHIm)]·$C_7H_8$ (left) with those of [Fe(TPP)(CO)(1-MeIm)]·$C_7H_6$ (center) and [Fe(TPP)(CO)(1,2-$Me_2$Im)]·$C_7H_8$ (right). Note the strong similarity in imidazole plane orientation between the left and right structures.

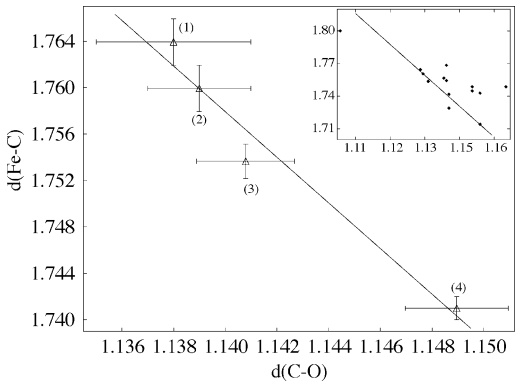


***Figure 8.*** Plot of Fe−C vs C−O distances (Å). Data illustrated in the main panel are (1) [Fe(TPP)(CO)(1,2-$Me_2$Im)], (2) [Fe(TPP)(CO)(1-MeIm)]·$C_6H_6$, (3) [Fe(TPP)(CO)(1,2-$Me_2$Im)]·$C_7H_8$, and (4) [Fe(TPP)(CO)(2-MeHIm)]·$C_7H_8$. Error bars are displayed. The linear fit has a correlation coefficient of $R = 0.98$.[93] The inset shows all iron(II) carbonyl imidazole structures, with the main panel correlation line overlaid.

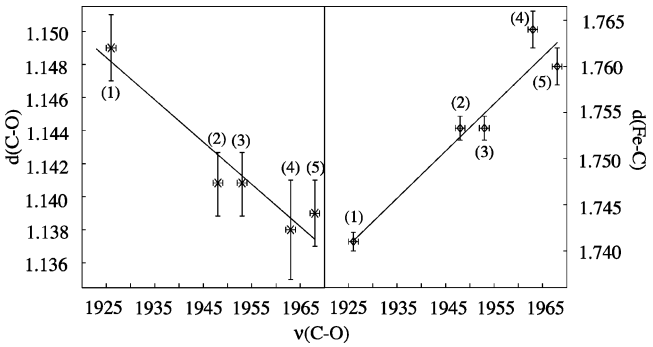


***Figure 9.*** Plots showing the relationship between the Fe−C and C−O distances (Å) and $\nu_{C-O}$ ($cm^{-1}$). The two panels show data for (1) [Fe(TPP)(CO)(2-MeHIm)]·$C_7H_8$, (2) [Fe(TPP)(CO)(1,2-$Me_2$Im)]·$C_7H_8$, (3) [Fe(TPP)(CO)(1,2-$Me_2$Im)]·$C_7H_8$ (second $\nu_{C-O}$), (4) [Fe(TPP)(CO)(1,2-$Me_2$Im)], and (5) [Fe(TPP)(CO)(1-MeIm)]·$C_6H_6$. Error bars are displayed. Correlation coefficients for both panels are $R = 0.96$.[93] A plot including all iron(II) carbonyl imidazoles is included in the Supporting Information.

likely hydrogen-bonded conformer. Although the exact interactions of CO in MbCO cannot be fully elucidated, the results we have observed for [Fe(TPP)(CO)(2-MeHIm)]·$C_7H_8$ further suggests that N−H interactions can cause large shifts in $\nu_{C-O}$ toward lower frequency akin to shifts observed from free heme (~1970 $cm^{-1}$) to $A_3$ in MbCO.

**Fe−C/C−O Bond Length Correlations.** Spectroscopic studies of a large number of protein and porphyrin systems with CO bound to iron(II) have shown that there is an inverse correlation of $\nu_{C-O}$ and $\nu_{Fe-CO}$.[5,10,61] This phenomenon is attributed to electron donation from the occupied iron $d_\pi$ orbitals to the empty $\pi^*$ orbitals on CO thus causing a reduction in the C−O bond order and a concomitant increase in the Fe−C bond order.[61] This classical $\pi$-back-donation effect should, in principle, lead to an inverse change in the Fe−C vs C−O bond distance. However, such bond-distance changes are typically too small to be reliably observed in single-crystal structure determinations. For the present structures, which have been determined at very high precision and accuracy, we find that the structural equivalent to the spectroscopists $\pi$-back-bonding inverse correlation for iron carbonyls can be observed.

A plot of the observed Fe−C vs C−O bond distances for the four structures is given in Figure 8; the data are shown in tabular form in Table 1. The inverse linear correlation is clear; the correlation coefficient of the fit, given by Pearson's $R$,[93] is 0.98. Values for all structurally characterized iron(II) carbonyl imidazole derivatives are shown in the inset of Figure 8. The linear fit correlation line from the main panel is overlaid on these data; the general fit to the correlation line is apparent. The larger range of values in the distribution of the data reflects the generally lower precision of the other measurements, as well as the possible presence of small systematic errors.

Not surprisingly, there are correlations between the measured, solid-state C−O stretching frequencies and the C−O and Fe−C bond distances in these four new derivatives. Figure 9 shows plots of $\nu_{C-O}$ vs the C−O bond distance (left panel) and $\nu_{C-O}$ vs the Fe−C bond distance (right panel). The increasing value of $\nu_{C-O}$ as the C−O distance decreases and the Fe−C distance increases can be clearly seen. The correlations for all equivalent literature data are given in Supporting Information Figure S5. The correlation fit lines from Figure 9 are imposed; although the general correlation may be recognized, the scatter clearly reflects the lower precision of most earlier structures. It should also be recognized that the correlations of Figure 9 are all based on tetraphenylporphyrin derivatives, while those of Figure S5 are principally those for tetraarylporphyrin derivatives that include many substituted-phenyls. There is very likely some porphyrin dependence (cis effects) on these correlations that will lead to differing trend lines. This is likely to contribute to some of the scatter in Figure S5.

**Axial Ligand Distortions: Structural Effects?** One early motivation for this study was the theoretical suggestion put

(93) A linear correlation coefficient, Pearson's $R$,[94] was used to judge the fit to the data.

$$R = \Sigma_i(x_i - \bar{x})(y_i - \bar{y})/\sqrt{\Sigma_i(x_i - \bar{x})^2}\sqrt{\Sigma_i(y_i - \bar{y})^2}$$

(94) Walpole, R. E.; Meyers, R. H.; Meyers, S. L.; Ye, K. *Probability and Statistics for Engineers and Scientists*, 7th ed.; Prentice Hall: Upper Saddle River, NJ, 2002; pp 391−394.

forward by Jewsbury et al.[22] that the possible distortions (bending/tilting) of the Fe−C−O group of myoglobin are the result of effects on the proximal (trans) side of the porphyrin plane. In this model, the off-perpendicular distortion of the Fe−C−O unit is caused by a nonequilibrium orientation of the proximal residue (histidine in the native protein) and not effects from the distal side. Our experimental test of this proposal was the preparation of a carbonyl complex with a sterically hindered trans imidazole ligand. A hindered imidazole would necessarily have a substantial off-axis tilt of the Fe−N bond that, if the Jewsbury hypothesis is valid, should then lead to some distortion of the iron carbonyl group.

The first such compound characterized was unsolvated [Fe(TPP)(CO)(1,2-$Me_2$Im)]. This complex crystallized in a monoclinic space group with required 2-fold symmetry along the axial bond direction. The Fe−N(imidazole) bond is indeed off-axis with a tilt of 6.2°; the required 2-fold symmetry leads to the disorder shown in Figure 2. However, the Fe−C−O unit is linear, as required by the imposed symmetry, with no evidence of disorder apparent in the thermal parameters. The imposed symmetry left some uncertainty in the result, and additional data were sought. Unfortunately, we were unable for some time to prepare appropriate crystalline materials to further study the question. Then, two related species were obtained nearly simultaneously.

Structure analysis for extremely high-quality crystals of the toluene solvates of [Fe(TPP)(CO)(1,2-$Me_2$Im)] and [Fe(TPP)(CO)(2-MeHIm)] became available. Crystals of [Fe(TPP)(CO)(2-MeHIm)]·$C_7H_8$ have a completely ordered imidazole; both complexes exhibit an off-axis Fe−N(imidazole) bond that does not seem to lead to any unusual distortions of the Fe−C−O unit. Indeed, the structural features associated with these Fe−C−O units do not display any more anomalous features than those observed in [Fe(TPP)(CO)(1-MeIm)]·$C_6H_6$, which has an unhindered imidazole. We conclude that any anomalous CO orientational effects (tilting and bending) do not follow the simple correlation pattern as suggested by Jewsbury et al.[22] Although there are some small Fe−C−O tilts in the three new compounds, they do not correlate directly with proximal ligand orientation and the pattern suggested by Jewsbury.

There does, however, seem to be an interesting relationship in the structural parameters involving the axial ligands. The effect was suggested from the [Fe(TPP)(CO)(1,2-$Me_2$Im)]·$C_7H_8$ result. As noted earlier, the axial 1,2-dimethylimidazole is disordered over two positions that are pseudo-2-fold related. The two ligand positions are slightly asymmetric with different Fe−N(Im) bond distances and nonequal site occupancies. Although correlation effects with such closely overlapped groups are difficult to define, all attempts to force equivalent Fe−N distances were unsuccessful. We believe that there are some differences in the two orientations. Final crystallographic results are shown in Figure S6 of the Supporting Information. Energetically, the major and minor imidazole orientations are probably only slightly different from each other. Nonetheless, the less-occupied orientation site not only has an unusually long Fe−$N_{Im}$ bond (2.143 Å) but also a C−Fe−$N_{Im}$ angle (168.6°) that is abnormally small. A search of the C−Fe−$N_{Im}$ angle for all other iron(II) carbonyl imidazoles in the literature showed that angles less than 173° had not been previously reported. This search did suggest that there is a relationship between values of the Fe−$N_{Im}$ bond length vs the C−Fe−$N_{Im}$ angle. Figure 10 displays these values for all iron(II) carbonyl imidazole porphyrinates that are not "strapped" or "capped." A decrease in the value of the C−Fe−$N_{Im}$ angle accompanies a lengthening of the Fe−$N_{Im}$ bond. These data points are fit linearly with a correlation coefficient of $R = 0.84$.[93] The inset of Figure 10 shows the values for all iron(II) carbonyl porphyrinates with imidazole as a sixth ligand reported to date; the correlation line from the main panel is superimposed.

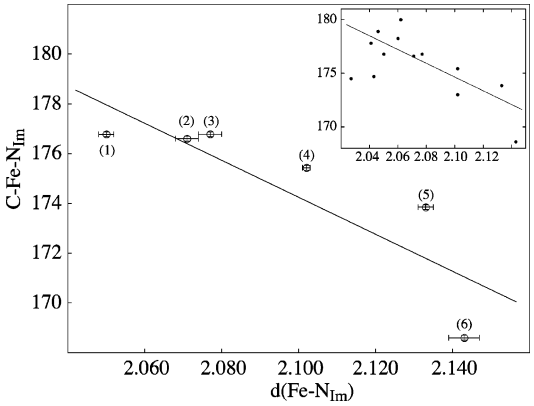


***Figure 10.*** Plot of the C−Fe−$N_{Im}$ angle vs the Fe−$N_{Im}$ distance (Å). All iron(II) carbonyl imidazole structures that do not contain a porphyrin strap are included (1) [Fe(TPP)(CO)(1-MeIm)]·$C_6H_6$, (2) [Fe(TPP)(CO)(1,2-$Me_2$Im)]·$C_7H_8$, (3) [Fe(OEP)(CO)(1-MeIm)], (4) Fe(TPP)(CO)(2-MeHIm)]·$C_7H_8$, (5) [Fe(TPP)(CO)(1,2-$Me_2$Im)], and (6) [Fe(TPP)(CO)(1,2-$Me_2$Im)]·$C_7H_8$ (minor orientation of the axial ligand). Error bars are displayed. The line showing the correlation has a correlation coefficient of $R = 0.84$.[93] The inset illustrates the values for all reported iron(II) carbonyl imidazole structures with the same correlation line as given in the main panel.

This correlation does suggest that proximal ligand pocket effects could have a role in the overall OC−Fe−histidine geometry in MbCO or HbCO. Any proximal ligand pocket effect that leads to modulation of the Fe−$N_{His}$ distance could be expected to affect the C−Fe−$N_{His}$ angle. What physiological role this effect may play is currently unknown. It is to be noted that distal pocket substitutions in many heme protein systems have been shown to affect ligand binding and discrimination; it is not difficult to imagine both distal and proximal control of ligand binding.

**Summary.** Four new six-coordinate iron(II) imidazole- and carbonyl-ligated porphyrinates have been prepared and characterized. Crystallographic data that were both of very high quality and high resolution were used in their structural characterization. Although the IR spectra of the four species showed similar values of $\nu_{C-O}$ in toluene solution, large differences (46 $cm^{-1}$ range) are seen in solid-state $\nu_{C-O}$'s. These frequency differences result from the differing crystalline environments of the CO. The lowest frequency (1926 $cm^{-1}$) is the result of a hydrogen bond to the CO oxygen. The structural data are of sufficient accuracy to allow the observation of the correlation of the Fe−C vs C−O distances that is expected from the classical picture of $\pi$ back-bonding for metal carbonyls. The Fe−C and C−O distances are also strongly correlated with the observed solid-state CO stretching frequencies. The off-axis tilting of the hindered imidazole ligand trans to CO appears to have little effect on possible tilts and bends of the Fe−C−O unit. However, there does appear to be a correlation between a decreasing C−Fe−$N_{Im}$ angle and an increasing Fe−$N_{Im}$ bond distance.

**Acknowledgment.** We thank the National Institutes of Health for support of this research under Grant No. GM-38401 (W.R.S). We thank Prof. Timothy Sage for useful discussions.

**Supporting Information Available:** Figures S1−S3, formal diagrams displaying the perpendicular displacement of core atoms from the 24-atom mean planes; Figure S4, diagram showing herringbone-like crystal packing pattern of [Fe(TPP)(CO)(1,2-$Me_2$Im)]·$C_7H_8$ and [Fe(TPP)(CO)(2-MeHIm)]·$C_7H_8$; Figure S5, plot illustrating Fe−C/C−O distances (Å) vs $\nu_{C-O}$ ($cm^{-1}$) for all carbonyl iron(II) imidazoles; Figure S6, ORTEP diagram of [Fe(TPP)(CO)(1,2-$Me_2$Im)]·$C_7H_8$ showing both orientations of the imidazole; Figure S7, displaying the environment of the oxygen atom in unsolvated [Fe(TPP)(CO)(1,2-$Me_2$-Im)]; Table S1, giving a summary of all crystallographic information; Tables S2−S25, giving complete crystallographic details, atomic coordinates, bond distances and angles, anisotropic temperature factors, and hydrogen positions for [Fe(TPP)(CO)(1,2-$Me_2$Im)]·$C_7H_8$, [Fe(TPP)(CO)(2-MeHIm)]·$C_7H_8$, [Fe(TPP)(CO)(1,2-$Me_2$Im)], and [Fe(TPP)(CO)(1-MeIm)]·$C_6H_6$; Table S26, orthogonal coordinates of the 1,2-dimethyl imidazole used in rigid body refinement of [Fe(TPP)(CO)(1,2-$Me_2$Im)] and [Fe(TPP)(1,2-Me2Im)]·$C_7H_8$; and crystallographic data available as CIF files. This material is available free of charge via the Internet at http://pubs.acs.org.

JA053148X